TECHNISCHE MECHANIK
European Journal of Engineering Mechanics
Diamond Open Access
journal homepage: www.ovgu.de/techmech

Tech. Mech., Vol. 46, Is. 1, (2026), 25–32
Received: 10.11.2025
Accepted: 10.02.2026
Available online: 16.02.2026

Influence of the Reynolds number and the axial fan impeller blade angle on the turbulent swirling jet flow

Novica Z. Janković[1]*, Đorđe S. Čantrak[1], Dejan B. Ilić[1], and Miloš S. Nedeljković[1]

[1] University of Belgrade - Faculty of Mechanical Engineering, Department of Hydraulic Machinery and Energy Systems, Kraljice Marije 16, 11120 Belgrade, Serbia

Abstract: An axial fan impeller, in-built as the case A, after ISO 5801, defined as "free inlet, free outlet" with nine twisted blades, serves as turbulent swirling flow generator for this study. Three-component laser Doppler velocimetry (LDV) measurements have been performed in the jet flow at ten measuring sections downstream the axial fan impeller outlet. This paper discusses distributions of the circumferential velocity downstream, due to its importance in the analysis of the turbulent swirling flow phenomenon in the jet. Gradients of the radial velocity are also discussed. Influence of the Reynolds number (defined by the fan rotation speed n), as well as impeller blade angle on the circulation distribution is the focus of this paper. It was shown that the values of the circulation in the domain $0 < r/R < 1$ decrease in hierarchical order from the initial (I) to the final (X) measurement section. However, this is not the case in the rest of the vortex jet flow, where the circulation changes are heterogeneous and chaotic, which is especially present in the domain $2 < r/R < 4$. The influence of the Reynolds number on the distribution of the circulation varies depending on the measurement section and r/R domain. It is shown that in the region near the axis, circulation doesn't depend on the impeller blade angle, while this influence is discussed in the rest of the flow region. Also, distribution of the angular velocity ($\Omega_W = W/r$) is considered. The influence of the blade impeller angle in one measurement section is presented as well. All these discussions lead to better understanding of the production of the Reynolds stresses in the generated turbulent swirling jet by the axial fan impeller.

Keywords: axial fan impeller, jet, swirling flow, turbulence, three-component LDV

1 Introduction

This paper presents the research of the turbulent swirling jet flow, generated by an axial fan impeller with twisted blades. This axial fan impeller is in-built in the installation following the setup category A for fans in the international standard ISO 5801 International Organization for Standardization (2017), which is defined as the installation with free inlet and free outlet. Experiments are performed by using the three-component laser Doppler velocimetry (LDV) system. An overview of the turbulent swirling flow jet experimental research is presented and discussed in Janković (2020), Janković (2017). In the paper by Pratte and Keffer (1972) is shown that the entrainment rate and angle of spread for the swirling jet was nearly twice as that of the non-swirling free jet. Study of jets with different initial swirl distributions is presented in Gilchrist and Naughton (2005). In this case, miniature five-hole probe is used for three-component velocity measurements. Experimental study on the effects of swirl on the development of an axisymmetric turbulent mixing layer is presented in Mehta et al. (1991). Single-component LDV measurements of the swirling flow generated by the guide vanes placed at the nozzle exit in the horizontal plane are reported in Sislian and Cusworth (1986). This paper studies the turbulent swirling flow in jets generated by the axial fan impeller with twisted blades. It is three-dimensional, inhomogeneous and anisotropic. Generated velocity field is very complex, characterized by inhomogeneity and distinct gradients, especially in the radial direction. Paper Janković et al. (2025) discusses development of the turbulent swirling flow velocity profiles in the axial fan jet for the same fan rotation speed $n = 1500$ rpm, while herein the influence of the Reynolds number (Re) and impeller blade angle (β_R) will be considered separately on the generated turbulence, although blade angle also influences the Reynolds number.

2 Experimental test rig

An axial fan impeller serves as a turbulent swirling flow generator. It has nine twisted blades with variable impeller blade angle at the outer diameter (β_R). It is designed after the law $rW = const$. Adjusted angles at the axial fan impeller outlet diameter, which is 0.399 m, are varied and have the following values: $\beta_R = 22°$, 26° and 30°. The dimensionless hub ratio, which represents the ratio of the hub and outer diameters, is 0.5, so this is a mid-pressure axial fan. The inner fan casing diameter is $D = 0.4$ m. The experimental test rig, with marked flow direction, is presented in Figure 1.
Three-component LDV measurements have been performed in ten measurement sections along vertical directions at a 10 mm distance each. Measuring sections along the axial fan rotating axis are $x = 300, 400$ to 2000 mm with a step of 200 mm, i.e. in the $x/D = 0.75D$ to $5D$ range, with the step $0.5D$, except for the first step $0.25D$. Figure 1 shows first five measuring sections. Three-component LDV system, by TSI, was used in these experiments. Continuum Ar-Ion laser of 5 W, by Coherent is applied. Two probes TSI TR60 with beam expanders XPD60-750 were used to form measurement volume. The TSI Flow Sizer software is

* E-mail address: djcantrak@mas.bg.ac.rs
doi: 10.24352/UB.OVGU-2026-004

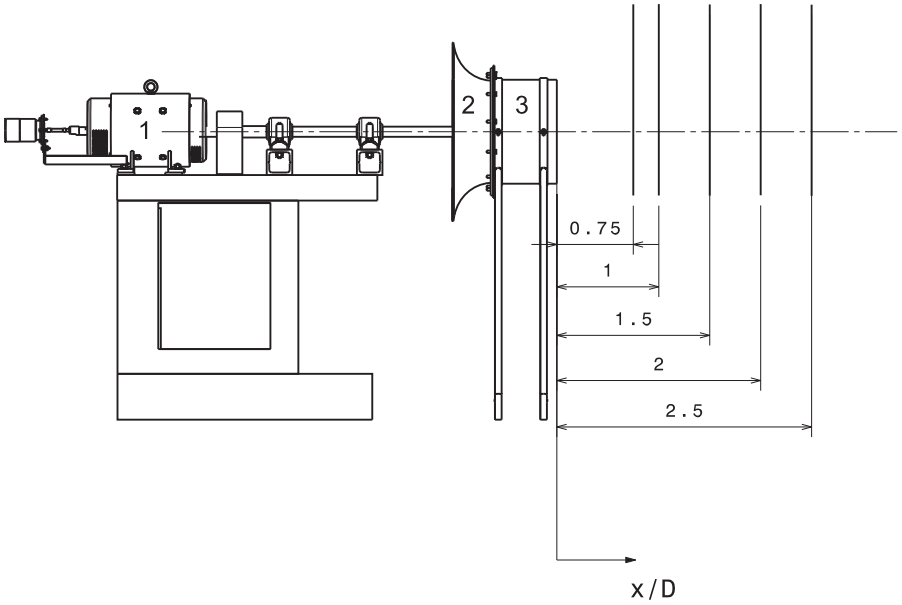

Fig. 1: Experimental test rig with marked measuring sections Janković et al. (2025): 1- DC motor, regulated with fully automated thyristor bridge with error up to ±0.5 rpm, 2- profiled bell mouth inlet and 3- axial fan impeller with casing.

used for acquisition and preliminary data analysis. The measurement focus with attached optics was 757.7 mm. Laser wavelengths were 514.5 nm, 488 nm and 476.5 nm. The measurement volume diameter was app. 70 µm, while measurement volume length was app. 280 µm. Both LDV probes work in a back scatter mode. The sampling interval is set to 20 seconds or one million samples taken (sampling stops when one of these two criteria is reached). Considering that the average sampling rate is from 1 to 2 kHz, it is clear that the time interval is the decisive criterion. The velocity was measured with uncertainty lower than 0.1 % Janković (2017). Uncertainty analysis of the used 3D LDV system is thoroughly analyzed and presented in Janković (2020), Ilić et al. (2019). Measurements have been performed for the axial fan impeller rotation speeds $n_1 = 1000$ rpm and $n_2 = 1500$ rpm. Flow seeding is provided by an Antari Z3000 fog machine loaded with the Eurolite Smoke Fluid. It was naturally sucked in the test rig by the axial fan. The fluid seeding is achieved in the following way: the fog machine is started 20 seconds before the start of the measurement in order to seed the laboratory space with particles. For each measurement position, the positions of the fog machine are determined in advance so as to obtain the maximum sampling rate.

3 Results and discussions

Experimental distributions of averaged velocities and circulations will be presented and discussed in this chapter.

3.1 Averaged velocities distributions

Experimentally obtained distributions of the total velocity magnitude along the jet axis, for $\beta_R = 30°$ and $n = 1500$ rpm, are presented in Figure 2. The flow development is observed. Namely, continuous deformation of the velocity profile with gradients in the axial and radial direction occurs. It is obvious that even 5D downstream a turbulent swirling flow still exists.
Circumferential velocity (W) significantly deforms profile of the axial velocity (U), as well as radial velocity (V), which is discussed for $\beta_R = 30°$ and $n = 1500$ rpm in Janković et al. (2025). Figure 3 presents radial-axial distributions of the velocity component W, i.e. in the non-dimensional form W/U_m, where U_m is the averaged velocity by area, in the turbulent swirling jet for $\beta_R = 30°$ and $n = 1500$ rpm, where $\varphi = 90°$ denotes upper half of the measuring section, and, consequently, $\varphi = 270°$ the lower half. They are obtained on the basis of the Reynolds averaging of the measured instantaneous velocity fields. It is shown in Fig. 3 that the development process is not finalized yet, that swirl is still present in all measuring sections and that the transformation in axial jet was not possible in the studied case.
With the increase of the axial coordinate x, the velocity W in the region $0 < r/R < 1$ decreases, so that the W - profiles, together with their max values W_{max}, are correctly hierarchically arranged in accordance with the order of the sections I-X. Outside this region, this is no longer the case, because the circumferential velocity profiles change their positions, i.e. "mix", and do not follow the order of the measurement sections. Figure 4 shows all three velocity components ($U_i = U, V$ and W) measured in the measuring section III, where $x = 600$ mm, for $\beta_R = 30°$ and $n = 1500$ rpm. Average velocity in this case is U_m =12.57 m/s, while Reynolds number is Re = 358951. Average circulation, calculated after the Eq. (1), is $\Gamma = 4.93$ m^2/s:

$$\Gamma = 4\pi^2 R^3 \int_0^1 k^2 U W \mathrm{d}k/Q \tag{1}$$

where $k = r/R$. Radial velocity (V) profiles in the turbulent swirling jet are characteristic [8]. It is important for convection and

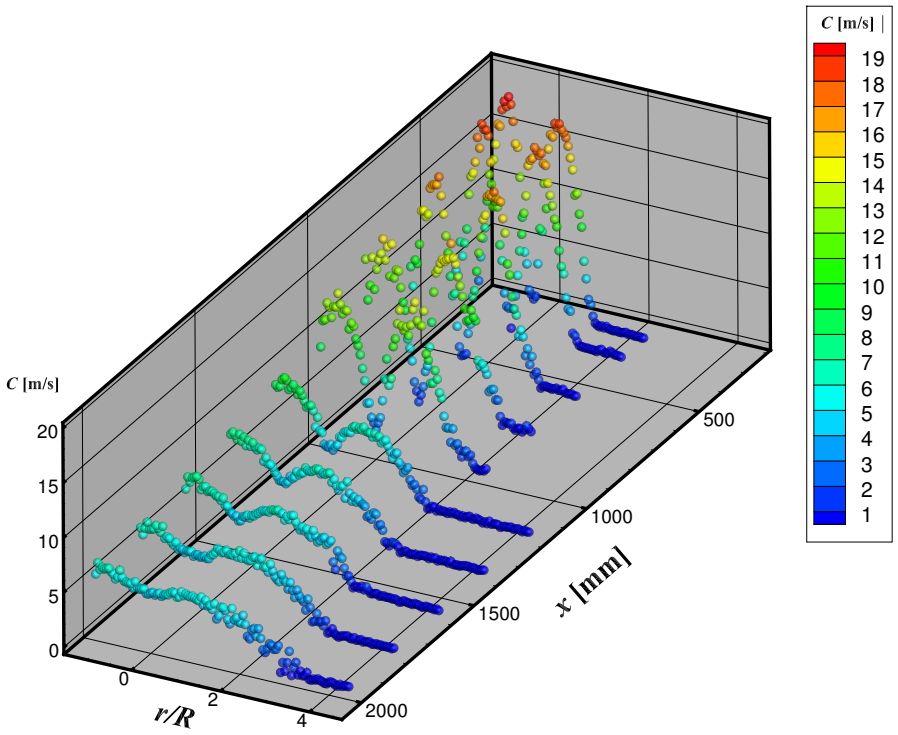

Fig. 2: Total velocity distributions $C = C(r, x)$ for $\beta_R = 30°$ and $n = 1500$ rpm Janković et al. (2025)

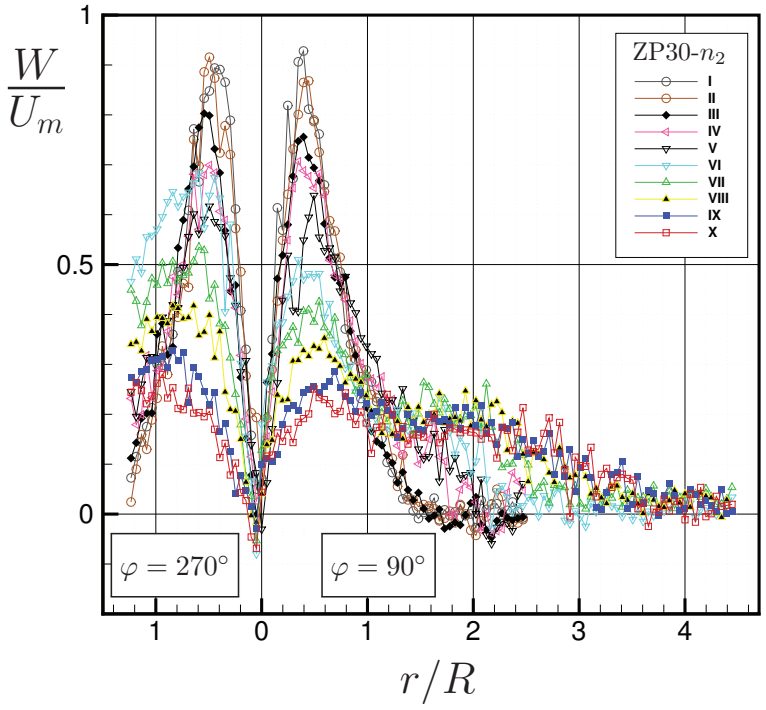

Fig. 3: Experimental radial-axial distribution of the circumferential velocity in the turbulent swirling jet for $\beta_R = 30°$ and $n = n_2 = 1500$ rpm Janković et al. (2025)

the occurrence of turbulent exchange to analyze the intensity and change in sign of the radial velocity, as also discussed in Janković et al. (2025). It is obvious that swirling flow changes the character of the radial movement, as well as intensities and signs of the derivative $\partial_r V$.

Gradient of the radial velocity is negative ($\partial_r V < 0$) in the vicinity of the axis, while in the domain $0.3 < r/R < 0.8$ this gradient is positive ($\partial_r V > 0$) (Fig. 4). Further increase of the radial coordinate, up to $r/R = 1.2$, results, again, in a negative gradient of the radial velocity ($\partial_r V < 0$). In the region with the higher radial coordinate, profile of the radial velocity becomes approximately

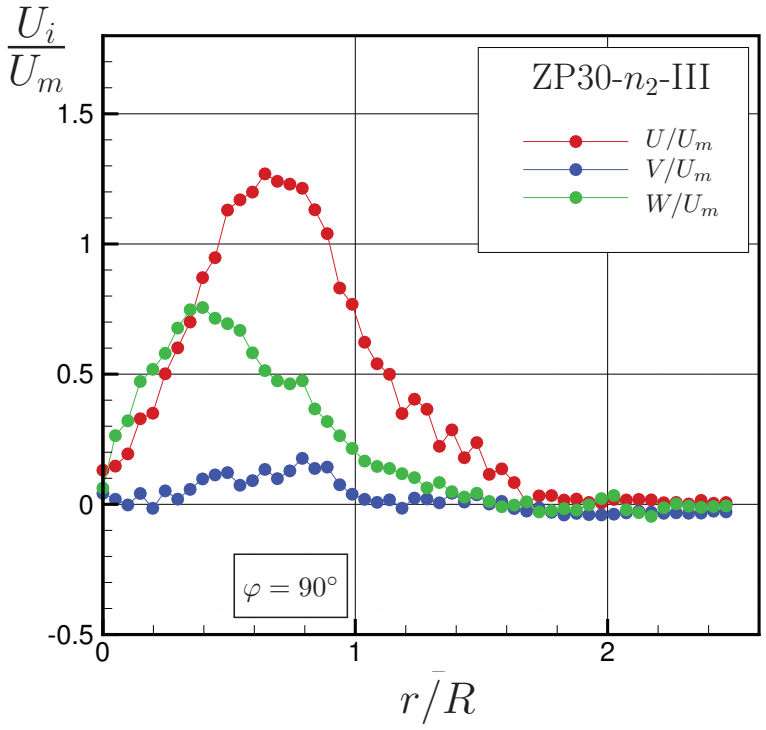

Fig. 4: All three velocities ($U_i = U$, V and W) distributions in the section III for $\beta_R = 30°$ and $n = n_2 = 1500$ rpm Janković et al. (2025)

uniform, so radial gradients $\partial_r V$ have lower values, and the change in its sign, when approaching the jet boundary occurs, with the predominant negative values. Experiments show that for characteristic points where maximum axial and circumferential velocities are reached, in all measuring sections, and also for this section III (Fig. 4) it stands: $r_{W-max} < r_{U-max}$. The presented empirical profiles of all three velocities show that in addition to the global maxima (within the respective sections), for example for section III (Fig. 4), U_{max} is reached for $r/R \approx 0.65$ and W_{max} for $r/R \approx 0.4$. Here, the number of local maxima for all three velocity components is also significant. The complexity of the structure of the averaged velocity field becomes even more obvious when to the previous elements is added the presence of heterogeneous changes of the $\partial_r U_i$ for all three components in the radial direction of the turbulent swirling jet, what is discussed in Janković et al. (2025).

3.2 Circulation distributions – influence of the Reynolds number

Figure 5 presents the experimental distribution of the circulation rW, i.e., its dimensionless form rW/RU_m. The complex structure is obvious.

The circulations in sections I-IV in the domain closer to the axis increase till $r/R \approx 0.5$ where they reach their maximum values, and then decrease as they move away from the axis. The first maximum values of circulation for the other sections are located somewhat further from the axis, but are in the domain $0 < r/R < 1$ and are less than circulation values in sections I-V. What is important to emphasize is that the values of the circulation in the domain $0 < r/R < 1$ decrease in hierarchical order from the initial (I) to the final (X) measurement section. However, this is not the case in the rest of the vortex jet flow, where the circulation changes are heterogeneous and chaotic, which is especially accented for $2 < r/R < 4$. In this domain, the circulations in sections VIII-X are even the largest, with the rW values having a smaller change from section VI to X than from section I to V. It is important to note, as can be seen in Fig. 5, that the largest initial circulations, i.e., the circulations in sections I to IV, have the largest negative changes in the radial direction . Negative values of circulation in measurement sections I to IV are achieved in the area of the cross section $1.5 < r/R < 2.4$, in accordance with the empirical distribution of the circumferential velocity W (Fig. 3). Experimentally obtained diagrams for $\beta_R = 30°$ in measurement sections I, III and V and two Reynolds numbers are presented in Fig. 6. These two values of Reynolds numbers are obtained for two different fan rotation speeds ($n_1 = 1000$ and $n_2 = 1500$ rpm).

The circulation maxima are concentrated around the value $r/R \approx 0.5$, while in the domain $0 < r/R < 0.55$ stands $\partial_r (rW) > 0$. In this area, the influence of the Reynolds number Re_2 is greater in sections I and III, while the influence of Re_1 on the circulation becomes slightly greater than the influence of Re_2 in section V. In the interval $0.55 < r/R < 1$, both influences are approximately the same, overlapping with a wide range. A more significant stratification of influences occurs in the domain $1 < r/R < 2$, where in section V the influence of Re_1 is greater than that of Re_2, which is also true for section III. With further increase in the radial coordinate, the influences are mixed, and the negative values of the circulation in the interval $1.5 < r/R < 2.4$ are more significantly influenced by the Reynolds number Re_2 than by the number Re_1.

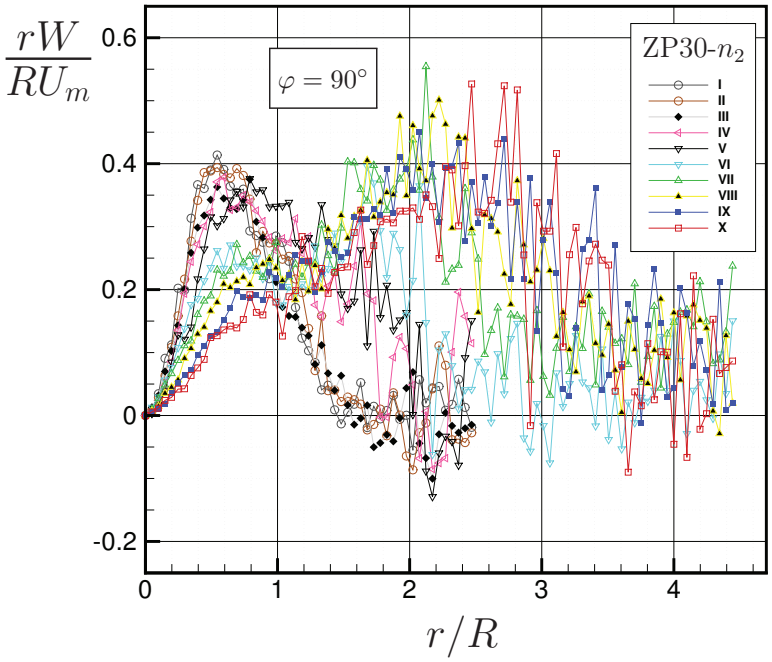

Fig. 5: Downstream development of the circulation in the vortex jet of the axial fan for $\beta_R = 30°$ and $n = n_2 = 1500$ rpm

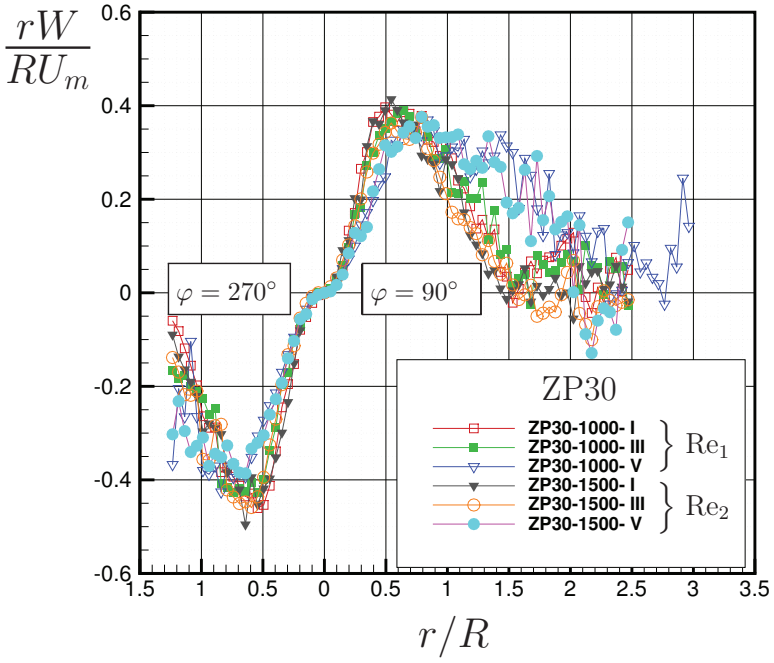

Fig. 6: The influence of the Reynolds number on the distribution of the circulation in sections I, III and V for $\beta_R = 30°$, $n_1 = 1000$ and $n_2 = 1500$ rpm

3.3 Circulation distributions – influence of the impeller blade angle

Figure 7 presents the experimental distribution of the circulation rW, i.e. its dimensionless form rW/RU_m for three various values of the impeller blade angle, i.e. $\beta_{R,i} = 22°, 26°$ and $30°$ ($i = 1, 2, 3$) and fan rotation speed $n = 1500$ rpm.

Experimentally obtained distributions for circulation, presented in Fig. 7, show that in the region near the axis, in the domain $0 < r/R < 0.4$, the profiles do not depend on the impeller blade angle. The curves reach their maxima at $r/R = 0.5$, and then, with increasing r, they decrease. It is obvious (Fig. 7) that almost in the whole region $0.5 < r/R < 2.5$, circulation has the highest values for $\beta_{R,2} = 26°$, except in almost all points in the region $0.5 < r/R < 0.9$ where higher values are obtained for $\beta_{R,3} = 30°$. The highest value of the circulation for the $\beta_{R,2} = 22°$ is obtained only in the point $r/R \approx 1.6$. The area of occurrence of negative values of rW is the same as in the previous cases (Figures 5 and 6), i.e. for $1.5 < r/R < 2.5$. It is necessary to emphasize in this analysis that the values of the empirical curve rW/RU_m, which determine the circulation changes in the radial and axial direction of the vortex jet, decrease at higher radial coordinates. This is indicated by Figures 5 and 6, and especially the experimental curve

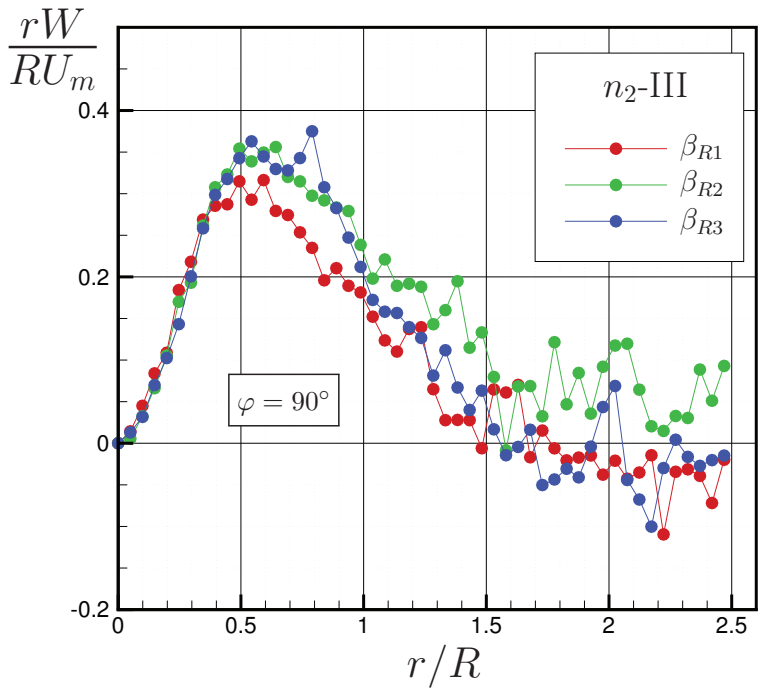

Fig. 7: Analysis of the influence of the blade angle $\beta_{R,i}$ (i = 1,2,3) on the behavior of the quantity $rW = f(r/R)$ in measurement section III of a vortex turbulent jet when $n = n_2 = 1500$ rpm

that determines the circulation during the operation of the axial fan with the impeller blade angle $\beta_{R3} = 30°$ affects the circulation in the domain $2.3 < r/R < 2.5$. The flow with a constant circulation $rW = const$ is obtained.

3.4 Angular velocity distributions

The quantity $\Omega_W = W/r$ and its changes, especially in the radial direction, play a major role in the analysis of turbulence and the influence of the generated vortex on the turbulent flow field in a swirling jet. This quantity characterizes rotational motion, i.e., the rotation of the fluid and determines the angular velocity. The radial experimental distributions of this quantity are shown in Figs. 8 and 9.

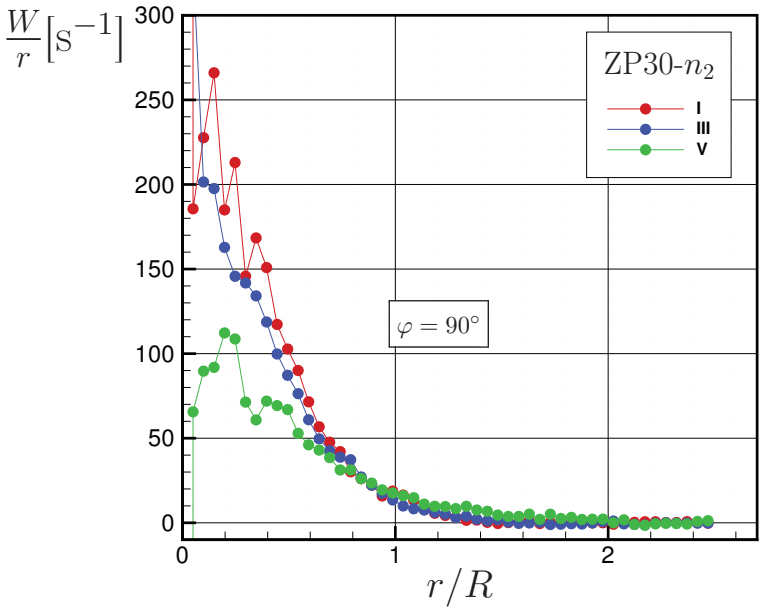

Fig. 8: Statistical – empirical distributions of the angular velocity for $\beta_R = 30°$ and $n = 1500$ rpm in three measurement sections I, III and V

Figure 8 presents changes of the W/r value in three characteristic sections of the jet for the $\beta_R = 30°$ and $n = 1500$ rpm. They are distributed in accordance with the experimentally obtained profile of the circumferential velocity W of the vortex generated in the given operating mode of the axial fan impeller. When the area in the immediate vicinity of the axis is excluded $r \to 0 \Rightarrow W/r \to \infty$,

then in sections I and V in the domain $r/R < 0.2$, the W/r function increases, so that at the measurement point $r/R \approx 0.1$ the maximum value $(W/r)_{max}$ is reached in section I, while in section V it is reached in the point $r/R \approx 0.2$. However, in the specified domain ($r/R < 0.2$) for section III, the function Ω_W decreases with increasing radial coordinate, which is the difference in relation to sections I and V. The mutual position of the curves Ω_W corresponds to the physics of the process, because the angular velocities are the highest in section I, lower in III, and lowest in the fifth section. This hierarchical order is maintained until $r/R < 0.8$, when the function W/r in the interval $0.8 < r/R < 2.3$ becomes slightly larger in section V, than the values in sections I and III. Figure 9 shows experimental curves, where i = 1,2,3, defines the influence of the impeller blade angle $\beta_{R,i}$ of the axial fan impeller on the generated vortex, which, as already shown, has a very complex structure.

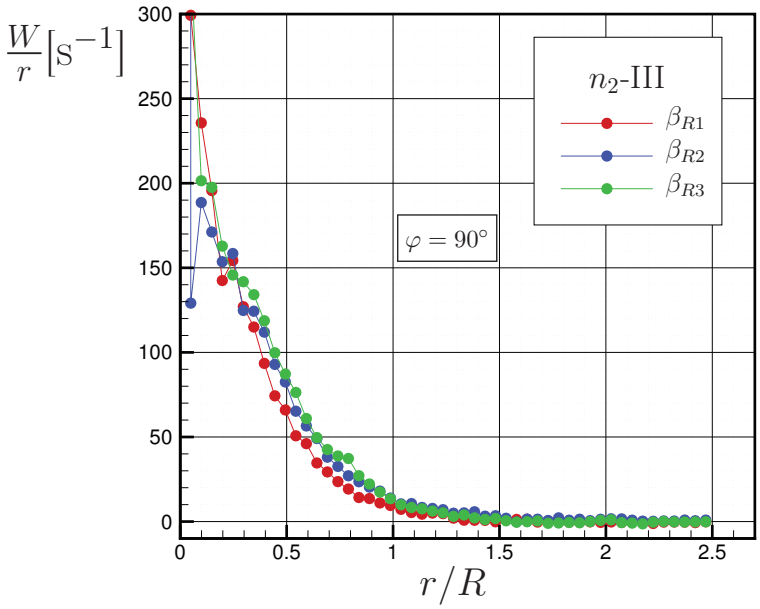

Fig. 9: The influence of the blade angle $\beta_{R,i}$ (i = 1, 2, 3) on the radial distribution of the quantity W/r in the cross section III of the fan jet for $n = n_2 = 1500$ rpm

It is normal that the influence of the angle $\beta_{R,3}$ is dominant, because it is larger than the other two angles $\beta_{R,1}$ and $\beta_{R,2}$ and this is especially expressed in the domain $0.15 < r/R < 1.1$. In the region around the axis, up to $r/R < 0.15$, the influence of the angle $\beta_{R,1}$ is larger than the influence of other two angles, while in the interval $1.1 < r/R < 1.5$, angle $\beta_{R,2}$ has a larger influence. For values of the radial coordinate $r/R > 1.5$, the influences of the angles $\beta_{R,i}$ on the angular velocity Ω_W are approximately the same. The decreasing character of the curves W/r is the same for all three angles. The role of the angular velocity Ω_W is very important in functions of the kind $\overline{u_i u_j}\partial_r W/r$. The distribution and gradient Ω_W provide a closer insight into the processes of turbulent exchange, as well as into the structure of turbulence in the flow field of a vortex jet. For example, the quantity $-\overline{vw}\partial_r(W/r)$ is responsible for the generation and distribution of the kinetic energy of turbulence in the jet flow region.

4 Conclusions

It could be summarized, on the basis of the previously presented experimental results and discussions, the following:

- Measurements have confirmed the assumption of the statistical axisymmetry of the velocity field (Figs. 2 to 4), which is important from both physical and mathematical point of view.
- Position of the circumferential velocity maximum is correlated with the vortex core diameter, as well as with the vorticity distributions. With increase of the axial coordinate (x) velocity W in the region $0 < r/R < 1$ decreases, so the circumferential velocity profiles are hierarchically distributed downstream from the section I to X. Outside this region this is not the case anymore, and W velocity profiles are mixed (Fig. 3).
- Experiments show that for characteristic points where maximum axial and circumferential velocities are reached, in all measuring sections (also for the Section III shown in Fig. 4) stands: $r_{W-max} < r_{U-max}$.
- It is shown that swirling flow changes character of the radial movement, as well as intensities and signs of the derivative $\partial_r V$ (Fig. 4).
- The values of the circulation in the domain $0 < r/R < 1$ decrease in hierarchical order from the initial (I) to the final (X) measurement section. However, this is not the case in the rest of the vortex jet flow, where the circulation changes are heterogeneous and chaotic, which is especially present in the domain $2 < r/R < 4$.
- The influence of the Reynolds number on the distribution of the circulation in sections I, III and V for $\beta_R = 30°$ varies depending on the measurement section and r/R domain.
- It is shown that in the region near the axis, in the domain $0 < r/R < 0.4$, circulation doesn't depend on the impeller blade

angle, while this influence is discussed in the rest of the flow region.

- It was shown that the biggest difference of the angular velocity ($\Omega_W = W/r$), measured in three different measurement sections, is in the domain up to $r/R \approx 0.8$, while not so obvious in the rest of the swirling jet flow region.
- The influence of the blade impeller angle in one measurement section is also discussed.
- All these discussions lead to better understanding of the production of the Reynolds stresses in the generated turbulent swirling jet by the axial fan impeller.

Acknowledgment and Funding Information

The results presented in this paper are the result of the research supported by the Ministry of Science, Technological Development and Innovation of the Republic of Serbia under the Agreement on financing the scientific research work of teaching staff at accredited higher education institutions in 2025, no. 451-03-137/2025-03/200105. The work on this paper is finalized during the student demonstrations in Serbia, which started in November 2024. and are still in progress and is dedicated to them who stand for the justice in our society.

References

R. T. Gilchrist and J. W. Naughton. Experimental study of incompressible jets with different initial swirl distributions: Mean results. *AIAA Journal*, 43(4):741–751, 2005.

J. T. Ilić, N. Z. Janković, S. S. Ristić, and Đ. S. Čantrak. Uncertainty analysis of 3d lda system. In *The 7th International Congress of the Serbian Society of Mechanics, Minisymposium M3: Turbulence, Proceedings*, Sremski Karlovci, Serbia, 2019. Paper No. M3j, p. 189.

International Organization for Standardization. Fans – Performance Testing Using Standardized Airways. Technical Report ISO 5801:2017, Geneva, Switzerland, 2017. https://www.iso.org/standard/56517.html.

N. Z. Janković. Investigation of the free turbulent swirl jet behind the axial fan. *Thermal Science*, 21(Suppl. 3):S771–S782, 2017.

N. Z. Janković. *Experimental and Theoretical Research of the Structure of Turbulent Swirl Flow in Axial Fan Jet*. Doctoral dissertation, Faculty of Mechanical Engineering, University of Belgrade, Belgrade, Serbia, 2020. (in Serbian), Hydraulic Machinery and Energy Systems Department.

N. Z. Janković, Đ. S. Čantrak, D. B. Ilić, and M. S. Nedeljković. Development of the turbulent swirling flow velocity profiles in the axial fan jet. In J. Vad, editor, *Conference on Modelling Fluid Flow (CMFF'25), Proceedings*, pages 397–402, Budapest, Hungary, 2025. Department of Fluid Mechanics, Faculty of Mechanical Engineering, Budapest University of Technology and Economics. Paper No. 65, ISBN 978-615-112-002-6, https://www.cmff.hu/papers25/CMFF25_Conference_Proceedings.pdf.

R. D. Mehta, D. H. Wood, and P. D. Clausen. Some effects of swirl on turbulent mixing layer development. *Physics of Fluids A: Fluid Dynamics*, 3(11):2716–2724, 1991.

B. D. Pratte and J. F. Keffer. The swirling turbulent jet. *Journal of Basic Engineering*, 94(4):739–747, 1972.

J. P. Sislian and R. A. Cusworth. Measurements of mean velocity and turbulent intensities in a free isothermal swirling jet. *AIAA Journal*, 24(2):303–309, 1986.